



## ARTICLE

# Analysis of Climate Change in the Area of Vojvodina-Republic of Serbia and Possible Consequences

Milan Gavrilović<sup>1</sup> Milan Pjević<sup>1</sup> Mirko Borisov<sup>1\*</sup> Goran Marinković<sup>1</sup>

Vladimir M. Petrović<sup>2</sup>

1. University of Novi Sad, Faculty of Technical Sciences, Trg Dositeja Obradovića 6, 21000 Novi Sad, Serbia

2. University of Belgrade, Institute of Chemistry, Technology and Metallurgy, Department for Ecology and Technoeconomics, Njegoševa 12, 11000 Belgrade, Serbia

### ARTICLE INFO

#### Article history

Received: 1 March 2019

Accepted: 23 March 2019

Published Online: 12 April 2019

#### Keywords:

Climate change

Vojvodina

Novi sad

Urbanization

Land surface temperature (LST)

NDVI

### ABSTRACT

Climate change conditions a wide range of impacts such as the impact on weather, but also on ecosystems and biodiversity, agriculture and forestry, human health, hydrological regime and energy. In addition to global warming, local factors affecting climate change are being considered. Presentation and analysis of the situation was carried out using geoinformation technologies (radar recording, remote detection, digital terrain modeling, cartographic visualization and geostatistics). This paper describes methods and use of statistical indicators such as LST, NDVI and linear correlations from which it can be concluded that accelerated construction and global warming had an impact on climate change in period from 1987 to 2018 in the area of Vojvodina – Republic of Serbia. Also, using the global SRTM DEM, it is shown how the temperature behaves based on altitude change. Conclusions and possible consequences in nature and society were derived.

## 1. Introduction

The current warming trend is of particular significance because most of it is extremely likely (greater than 95 percent probability) to be the result of human activity since the mid 20th century and proceeding at a rate that is unprecedented over decades to millennia.

The world is undergoing the largest wave of urban growth in history. At present, more than half of the world's population is living in urban areas such as towns and cities, and it is expected that by 2030 this number

will increase to about 5 billion (UNFPA)<sup>[16]</sup>. There are 7,163,034 inhabitants in Serbia, of which 2,914,990 or 40.5% of the population live outside of urban settlements, and this number is constantly falling due to the transition from rural areas to urban areas. An increase in number of people moving from rural areas to urban areas has further influenced the climate change of major cities in Serbia.

Novi Sad ranks 2nd in terms of population and is the most urbanized city of Serbia with 341,625 inhabitants of which 277,522 live in urban areas. It has a relative high population density with 486 persons per sq km. This may

\*Corresponding Author:

University of Novi Sad,

Faculty of Technical Sciences, Trg Dositeja Obradovića 6, 21000 Novi Sad, Serbia;

Email: mborisov@uns.ac.rs

be attributed to the fact that this city will be the European Capital of Culture in 2021, which will be the first time that this prestigious title bears a city from the country that is a candidate for EU membership. In addition to this, Novi Sad is a rapidly growing city and is also famous as a tourism destination among the masses. Therefore, as the industry and tourism sectors grow, the growth of service sector also accelerates, accentuating population growth. To accommodate this growing population, urban areas will further increase thus taking a toll on the natural resources. The study presented here gives an insight into the changing vegetation and temperature patterns of city Novi Sad and its surrounding areas due to increase in urbanization.

Estimates based on climate modeling, according to moderate scenarios, indicate that the annual temperature in Serbia will increase by 2.6 degrees Celsius by the end of the century. The heating will not be even during the year. The temperature of summer will increase by 3.5 degrees Celsius, autumn by 2.2, winter by 2.3, and spring by 2.5 [12].

NDVI is considered as an excellent indicator of vegetation density and is the most commonly used vegetation index. NDVI represents useful tool which can amalgamate vegetation, ecosystem, climate and environment and perform studies at large spatial and temporal scales [11].

The thermal infrared (TIR) band on the Landsat satellites is useful for calculating the LST. LST is defined as the interface temperature between the Earth's surface and its closest atmosphere, and therefore is a key variable for understanding the interaction between the earth and the atmosphere [16]. The correlation between the LST and vegetation indexes, such as NDVI has been documented. Mallick et al. (2008) examined the relationship between NDVI and LST using Landsat data and found strong relationship between these two variables.

In the present study, NDVI has been used to derive LST [19]. Also, using statistical calculations, a correlation between the NDVI index and the LST is determined, and in which linear relationship the two values are interrelated (regression). Based on this, it is shown how altitude change using SRTM DEM and construction expansion influences temperature change.

## 2. Study Area and Data Used

Novi Sad is located at 45° 20' 00" N, 19° 51' 00" E, in the central part of the Autonomous Province of Vojvodina, in the north of Serbia, at the border of Backa and

Srem (Figure 1). The city covers an area of 702.7 square kilometers, at an altitude of 80 meters. According to the final results of the population census in 2011, there were 341,625 inhabitants in the administrative territory of the city of Novi Sad, while 277,522 inhabitants live in the urban area of the city of Novi Sad. On the left bank of the Danube there is a plain part of the town (Backa), while the hilly part of the city (Srem) is located on the right bank, on the slopes of Fruška Gora.

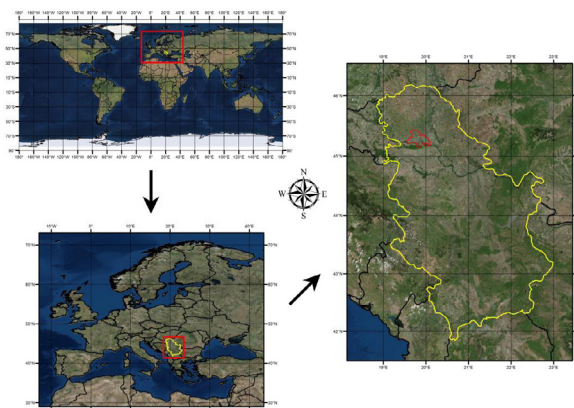


**Figure 1.** Location map of municipality of Novi Sad

Two Landsat images have been used for this study. The detail of the data used is given in Table 1.

**Table 1.** Specifications of Landsat data used in the study

Satellite/Sensor	Acquisition Date(s)	Bands used	Spectral Wavelength (µm)	Spatial Resolution (m)
Landsat-5/TM	25 Aug. 1987	Red (B3)	0.63-0.69	30
		Near-infrared (B4)	0.76-0.92	30
		Thermal infrared (B6)	10.40-12.50	120
Landsat-8/OLI-TIRS	30 Aug. 2018	Red (B4)	0.64-0.67	30
		Near-infrared (B5)	0.95-088	30
		Thermal infrared 1 (B10)	10.60-11.19	100 <sup>1</sup>
		Thermal infrared 2 (B11)	11.50-12.51	100 <sup>1</sup>

## 3. Methodology

<sup>1</sup> TIR/TIRS bands are acquired at 120/100 m resolutions, but are resampled to 30 m in delivered data product

### 3.1 LST Determination from Remote Sensing Images

To obtain LST from satellite sensors based on TIR measurements, radiometric calibration, emissivity and atmospheric corrections are required [8].

The Landsat OLI-TIRS had two bands - band 10 and 11 - but only band 10 was used here. Therefore, this study uses single-window based algorithm for NDVI to obtain land surface emissivity (LSE). From the various approaches given in the literature [19][20], modification of the NDVI Thresholds Method (NDVI THM) [20] is used here. The following steps are followed to obtain LST from thermal images and NDVI images.

#### 3.1.1 Calculation of Radiance Images

The raw digital number (DN) values of TM have been converted to radiance using the formula given by Chander et al., (2009):

$$L^* = \frac{(L_{max} - L_{min})DN + L_{min}}{DN_{max}} \quad (1)$$

where  $L^*$  is the spectral radiance received at the sensor;  $L_{min}$  and  $L_{max}$  are the minimum and the maximum spectral radiance for the sensor respectively;  $DN_{max}$  is the maximum DN. For TIRS, the following formula is used:

$$L^* = M_L \times DN + A_L \quad (2)$$

where  $M_L$  is band specific multiplicative rescaling factor and  $A_L$  is the band specific additive rescaling factor from the metadata.

#### 3.1.2 Calculation of Radiant Temperature

Radiance images derived from thermal bands were used to calculate the radiant temperature using the formula [2]:

$$T_r = \frac{K2}{\ln\left(\frac{K1}{T_r} + 1\right)} \quad (3)$$

where  $T_r$  = radiant temperature (in Kelvin);  $K1$  and  $K2$  = pre-launched calibration constants 1 and 2 respectively ( $W / (m^2 \text{ sr } \mu m)$ );  $L^*$  = spectral radiance.

### 3.2 Creation of NDVI Images

NDVI is first conceived by Rouse et al. (1973) and it is based on the absorption of light by vegetation in the red band and its reflectance in near-infrared band [4]. The value of NDVI ranges from -1 to +1 where -1 represents pixels having no vegetation and +1 pixels with dense vegetation. Values greater than 0.6 indicate the presence of thick green vegetation. As the values are closer to 1, the vegetation is denser. The range of values from 0.2 to 0.5 corresponds to low vegetation. Areas without vegetation have values close to zero, while negative values corre-

spond to desert areas, water, clouds, snow covered areas, etc. NDVI can be expressed as [18]:

$$NDVI = \frac{NIR - Red}{NIR + Red} \quad (4)$$

where, NIR is the reflectance of near infrared band and R is the reflectance of red band.

### 3.3 Calculation of Emissivity

The emissivity of surface varies with vegetation, soil moisture, roughness and viewing angles. Three major methods are recommended in literature for LSE estimation for LST inversion [3]:

- (1) classification- based emissivity method (CBEM),
- (2) NDVI- based emissivity method (NBEM) and
- (3) day/night temperature- independent spectral indices-based method [22].

NDVI was classified in three classes:

- (1) bare soil:  $NDVI < 0.2$ , (b.),
- (2) mixture of bare soil and vegetation:  $0.2 \leq NDVI \leq 0.5$  and (C.),
- (3) fully vegetated:  $NDVI > 0.5$ .

LSE for each of these classes is estimated using the following equation [10][22]:

$$\epsilon_i = \begin{cases} a_i p_{red} + b_i & NDVI < 0.2 \\ \epsilon_{v,i} p_v + \epsilon_{s,i} (1 - p_v) + C_i & 0.2 \leq NDVI \leq 0.5 \\ \epsilon_{v,i} + C_i & NDVI > 0.5 \end{cases} \quad (5)$$

Where,  $p_{red}$  is the reflectance of red band,  $p_v$  is the fraction of vegetation,  $\epsilon_s$  and  $\epsilon_v$  is the emissivity of soil and vegetation and  $a_i$ ,  $b_i$ ,  $C_i$  are the essential coefficients which are discussed in Yu et al. (2014).

Sobrino et al., (2004) considered 49 soil spectra included in the ASTER spectral library and obtained the following expression for deriving LSE from pixels having proportion of both soil and vegetation:

$$\epsilon = 0.004p_v + 0.986 \quad (6)$$

where  $p_v$  - vegetation proportion and can be derived from NDVI image according to the equation given by Carlson and Ripley, (1997):

$$p_v = \left[ \frac{NDVI - NDVI_{min}}{NDVI_{max} - NDVI_{min}} \right]^2 \quad (7)$$

where  $NDVI_{max} = 0.5$  and  $NDVI_{min} = 0.2$ . The values 0.5 and 0.2 are used for scenes which have the presence of bare soil and vegetation respectively. It has been reported that this equation is the most suitable if there is a presence of bare soil and vegetation in a pixel, which is the case in the study area.

### 3.4 Calculation of LST

LST refers to the temperature of the surface layer of the soil. It differs from air temperature (temperature obtained within the weather report). LST depends on the albedo

(the measure of the reflection of the sun's radiation from the surface of the Earth), the vegetation cover and the humidity of the soil. The outputs derived from  $T_r$  and  $\epsilon$  have been then used as inputs to calculate the LST using the following formula<sup>[21]</sup>:

$$LST = \frac{T_r}{1 + \left(\frac{\lambda T_r}{\rho}\right) \ln \epsilon} \quad (8)$$

where  $\lambda$  = central wavelength (in  $\mu\text{m}$ ) of the Landsat thermal band;  $\rho = 1.438 \cdot 10^{-2\text{m}}$  K.

The NDVI and LST images thus derived have been used to study the spatio-temporal pattern.

### 3.5 Statistical Analysis Methods

Correlation represents the interconnection between different phenomena represented by values of two variables. Linear correlation coefficient, as a relative measure, takes values from -1 to +1. If it takes positive values, the correlation between phenomena is either direct or positive (both phenomena show dichotomous variations). In the case where the correlation coefficient  $<0$ , the relationship is inverse or negative (when one phenomenon increases the other decreases, and vice versa). If there is a functional connection between the observed phenomena (all the empirical points are right on the right line), we are talking about perfect correlation. Then the coefficient of correlation takes the value -1 (if the connection is inverse) or +1 (if the connection is direct). When correlation coefficient in absolute value is closer to 1, the stronger is the correlation between the phenomena. On the contrary, the closer the linear connection is to zero the weaker is connection.

On the basis of the large number of samples examined, we cite a "rough" division of correlation coefficient values:

- (1)  $>0.70$  is considered a strong connection,
- (2)  $0.30-0.69$  is considered to be a central connection,
- (3)  $<0.30$  no linear connection (does not exclude the existence of a nonlinear form of connection).

## 4. Results and discussion

Analysis of the results obtained requires a certain experience in the field of processing and interpretation of satellite images. The analysis represents a step between the processing of the image and a complete understanding of the results obtained and it makes it an instrumental in the complete process. The methods of analysis were visual and statistical.

The analysis itself begins with getting to know the target area, which in this case is the area of the municipality of Novi Sad. For analysis in this article satellite images were taken from August 25, 1987 (Figure 2) and from August 30, 2018 (Figure 3). The first step is a visual analysis

of two images displayed in the true color combination of colors, in order to represent changes in Novi Sad.

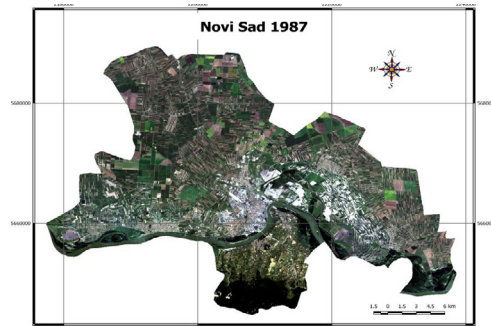


Figure 2. Display of the image from 1987 in the true color combination

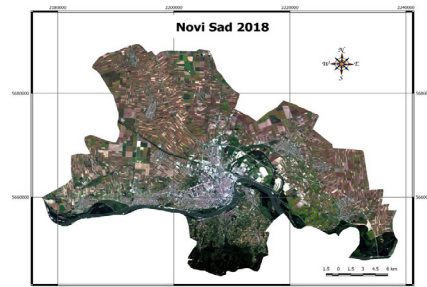


Figure 3. Display of the image from 2018 in the true color combination

From the shown, it can be seen an increase in the construction in the western part of the city of Novi Sad towards Futog and the northern part of the city of Novi Sad, ie the settlement of Klisa, as well as the expansion of the neighboring settlement Rumenka. The city was also built in other areas, but the changes in these areas are the most obvious, thus pointing to potential characteristic results after the application of certain processing methods.

The next step is a confirmation of previously observed conclusions through formal analysis. First, the temperature values at the Earth's surface were calculated, for both data sets, using the LST index according to the above formulas. The obtained results are shown in Figure 4 and Figure 5.

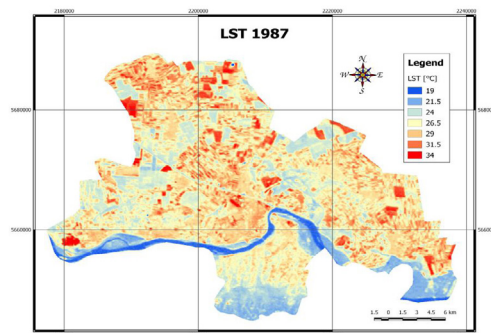


Figure 4. LST index for 1987 image

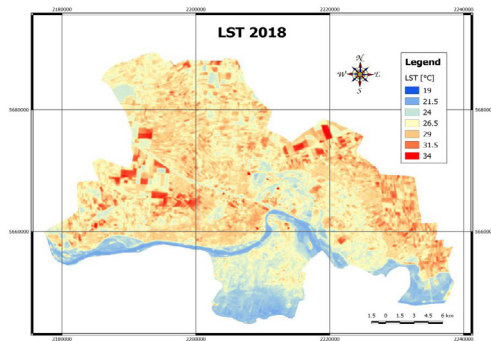


Figure 5. LST index for 2018 image

From the previous two images (satellite images from 2018) it can be seen the increase in the temperature of the surrounding agricultural land. Further, the minimum, maximum and mean temperature values in this area are analyzed, as well as the land in the western and northern part of the city of Novi Sad, where in this period of 31 years there has been intensive construction and expansion of the city. By inspecting the obtained numerical data (Table 2), the conclusion was made that in the period of 31 years the average temperature increased by 0.14 degrees. At the maximum value, it can be seen that the temperature in this period decreased by 0.59 degrees. The most interesting data is the one obtained for the minimum temperature, from which can be seen that the minimum surface temperature of the earth has increased by 1.99 degrees Celsius.

Table 2. The table of extreme and mean values of the LST index

Acquisition Date(s)	Min	Max	Mean
25 Aug. 1987	19.29	35.67	26.81
30 aug 2018	21.28	35.08	26.95

In order to better understand the obtained results, for the 500 arbitrarily selected points (which are correctly distributed in this test area) on which the temperature values were read, the histograms for both analyzed periods were formed (Figure 6 and Figure 7).

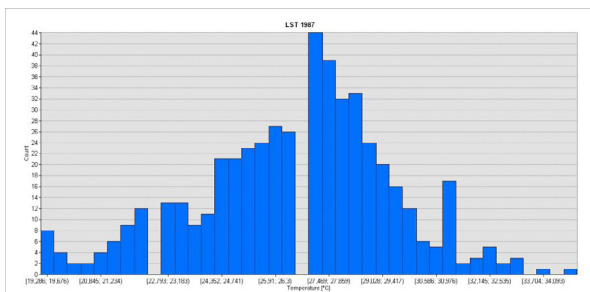


Figure 6. Histogram value for LST index for 1987 image

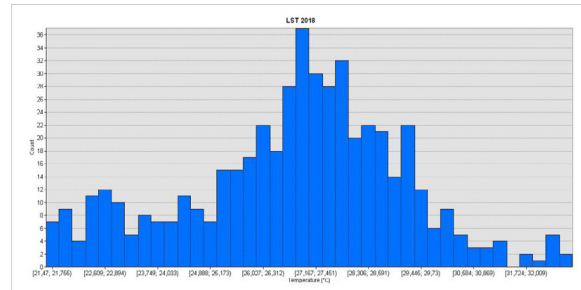


Figure 7. Histogram value for LST index for 2018 image

What clearly can be seen from above presented histograms is a much higher number of peaks with higher temperatures for image from 2018 than for the one from 1987. However, it can be stated with certainty that in this area, during the period of 31 years, there has been land warming, which is due to various factors such as global warming, urbanization and construction, etc.

High temperature areas also typically have lower NDVI values. This aspect has also been corroborated from the analysis of the relationship between LST and NDVI. There is an obvious correlation between NDVI and LST from the visual interpretation of NDVI and LST. In LST figures, the LST values of non-vegetated areas (built, infertile, dried riverbeds) are greater than those obtained for areas related to water bodies and vegetation, including agricultural land (Figure 4 and Figure 5). Values are opposite to NDVI images (Figure 8 and Figure 9). In order to study the variance of NDVI and LST, the pixel values of NDVI and LST that were derived show that LST peaks are usually in areas in which buildings are located, while the basins are mainly where water bodies and vegetation are located. NDVI peaks occur in vegetation areas, including agricultural land. So, NDVI and LST show an apparent negative correlation. In other words, the NDVI values are low (or even negative) where LST is high and vice versa. This is characteristic for both analyzed periods.

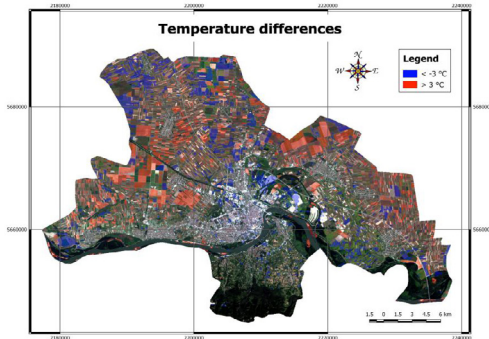


Figure 8. Correlation curves of NDVI and LST images of the 1987 year



Figure 9. Correlation curves of NDVI and LST images of the 2018 year

In order to prove how the urbanization and expansion of the city, ie, the construction of new buildings has an effect on the temperature increase, as well as to examine whether and how accurately the newly built objects can be detected on the basis of soil temperature changes, the following analysis was made. First, the temperature difference from 2018 and 1987 was calculated, and then only the values with a difference greater than 3 degrees Celsius for the given area were shown. The result is shown on the following chart (Figure 10).



**Figure 10.** Difference temperature greater than 3 degrees Celsius

From the following picture (Figure 11) we can clearly see that the temperature at which the object was built has increased. As temperature of objects are more in relation to the soil temperatures, it comes to the conclusion that all the places where the new buildings were built can be clearly detected.

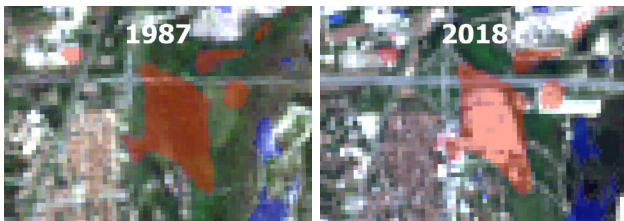


**Figure 11.** Detection of built objects

However, the problem occurs in places where there has been a change in the use of agricultural land. The problem case is shown in the following figure (Figure 12).

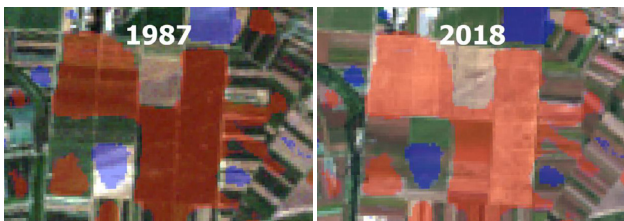


**Figure 12.** Error in the detection of built objects

Here it can be seen that on image from 2018 the area

is covered with green vegetation, which is not the case in the 1987 image. Due to this fact, various soil temperatures occur, i.e. The land without vegetation is heated more and vice versa. Therefore, in all places where there has been a change in the use of agricultural land, a significant change in temperature will occur, and such places will be detected. Precisely because of everything previously explained, this method for detecting built objects can not be considered reliable.

As the municipality of Novi Sad has mostly plain area, which is largely represented, and part of Fruska Gora, which has a much higher altitude than the surrounding area, the question is how the altitude change affects the temperature of the land.

By examining next graph (Figure 13), which was formed on the basis of the previously created 300-point test model and for which the heights of the SRTM DEM are read, with the rise in height, considerably fewer oscillations in temperature variations appear. Thus, the temperature difference values for the plain part range from -10 to +9, and as the height rises, this interval decreases to 2 degrees. It should also be taken into account that the Fruska Gora National Park is a special nature reserve and that construction is not permitted in that part. Therefore, due to the fact that there is no change in the use of land in that part, there are no significant changes in temperature.

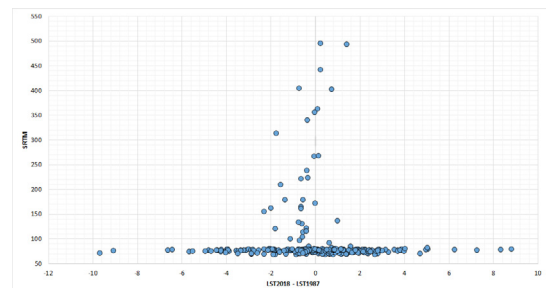


**Figure 13.** Changing temperature depending on height

Further analysis refers to temperature analysis for 10 characteristic locations. The coordinates of these points are given in Table 3. The spatial distribution of these points is shown in Figure 14.

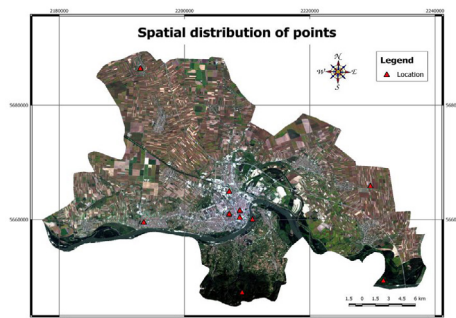


**Figure 14.** Spatial distribution of point

It can be seen that data are collected from points located on different land use/land cover classes, such as built areas, vegetation areas, water bodies, reefs/open areas, for better representation.

**Table 3.** Test model and coordinate values and temperatures on them

Name	Latitude	Longitude	DEM	LST 1987	LST 2018	LST 2018 - 1987
Dunav	45°14'40.70"	19°51'38.10"	70.0	19.2861	21.7918	2.5058
Fruška Gora	45°09'47.58"	19°50'43.90"	416.0	21.9456	22.2635	0.3179
Stadium	45°14'48.27"	19°50'32.37"	74.0	29.6049	28.2021	-1.4028
Park	45°15'01.53"	19°49'37.28"	78.0	25.8325	25.5115	-0.3210
BIG	45°16'31.61"	19°49'37.79"	77.0	27.1030	32.1886	5.0856
Theater	45°15'15.72"	19°50'32.59"	82.0	30.8398	30.9707	0.1309
Futog	45°14'29.26"	19°42'16.38"	80.0	28.3600	28.6678	0.3078
Stepanovićevo	45°24'40.61"	19°41'58.90"	79.0	27.5229	27.2127	-0.3102
Field	45°16'53.56"	20°01'46.42"	77.0	32.4672	31.9203	-0.5469
Coast of the Dunav	45°10'36.70"	20°02'53.42"	75.0	21.9455	23.8695	1.9239

To better understand soil temperature variation, a graph is given (Figure 15), for which for each characteristic location the obtained LST temperature values for both analyzed periods in the form of bar graphs are displayed. From the table and from the graph shown, it can clearly be seen that the greatest increase in temperature is at the site of the BIG shopping center, which occupies a large area and which has a large parking lot, and as there were no objects in that place in 1987, this result is very logical. At locations representing arable land and parks, we even see a decrease in the temperature for small values. It is also interesting to note that the value of the Danube and narrow band along the river has increased.

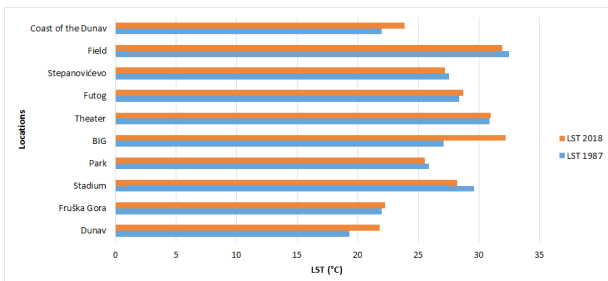


**Figure 15.** Comparative analysis of temperature values for each point

Healthy vegetation represents power and greenery that can be directly linked to NDVI, as well as conditioning the crops. The high values of NDVI are shown as crops,

orchards and forests as a result of a high level of green biomass, while low NDVI values represent a bare ground and urban area. The scatter graph was generated for both periods, for a previously created 300-point test model for which the results of the obtained NDVI and LST indexes were read (Figure 16 and Figure 17). Figure 16 shows the dependence between LST and NDVI index for 1987, and on Figure 17 is the dependence between LST and NDVI index for 2018.

As previously stated, the values of the  $R^2$  coefficient range from 0 to 1 and tell us how many variables (NDBI, LST) are dependent on one another. If  $R^2 = 0$  there is no linear connection and the variables are independent. The  $R^2 \sim 1$  linear bond between the variables is stronger. Variables in linear equations are: Y - LST, X - NDVI,  $R^2$  - determination coefficient.

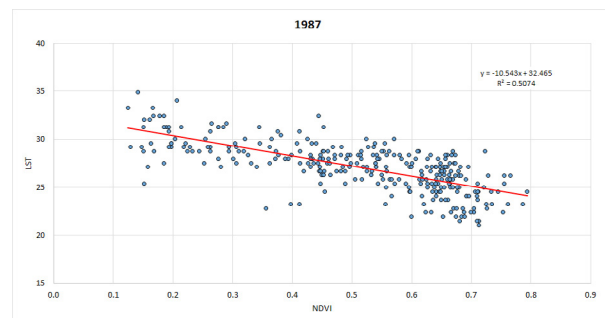


**Figure 16.** Scatter plot between LST and NDVI for 1987

As we see on the first chart for 1987, LST has a negative correlation with NDVI ( $R^2 = 0.51$ ). for agricultural land. This is further taken from labor and changes slightly: It means an area that has more vegetation is having low temperature because the available energy is parting more towards the evapotranspiration process, so that LST will be lesser as compared to the low vegetation area. Scanty vegetation also has higher LST due to low NDVI value.

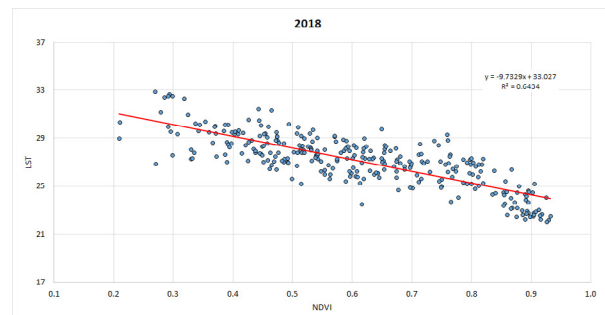


**Figure 17.** Scatter plot between LST and NDVI for 2018

From the second graph from the data obtained for 2018 we see that LST as in the previous case has a negative correlation with NDVI ( $R^2 = 0.64$ ).

## 5. Conclusion

First, it is important to clarify that climate change differs from global warming. This is a mistake made by many, especially the public. Although many aspects of climate change relate to heating problems, this concept also covers other complex climatic conditions. Regardless of their nature, the role of human activities in this climate change is certainly a matter of great concern. For example, anthropogenic global warming is simply an expression that is used for global warming caused by human activity.

In recent decades, climate change has become a major theme in the world. Over the past century, global temperatures have increased by 0.8 °C, since the CO<sub>2</sub> concentration in the atmosphere has increased from 280 to 370 ppm: it is expected to double to 2100, followed by a temperature rise of 1.1-5.4 °C above the 1900 level (IPCC, 2007).

In fact, most recorded global warming has occurred over the past four decades, and 2016 and 2017 have been certified as the hottest years of record. If this continues to increase, as is expected in urban areas, in particular, we should testify to serious cases of urban overheating scenarios.

This also causes changes in existing weather patterns, including increased frequency and size of drought, floods and other extreme weather conditions<sup>[5][6]</sup>. These changes are mainly attributed to the increased human exploitation of natural resources, especially fossil fuels (the release of greenhouse gases into the atmosphere), but also to industrialization, forest degradation and urbanization affecting the nature of landscapes (IPCC, 2007). We defined urbanization as a substitute for nature by culture<sup>[14]</sup>.

Climate change is being perceived as the greatest challenge of this era. Anthropogenic (ie Human) activities were the main factor in global warming, which led to a change in weather patterns, which in turn exacerbated socio-cultural issues such as hunger, drought and the rise in sea levels that led to mass migration and demographic displacement.

In the context of the urban environment, "urban" includes not only the city center, but also the surrounding suburbs, urban greenery, industrial areas and rural-urban edges<sup>[13]</sup>. This is a growing and inevitable phenomenon: in 1960, 60% of the world's population lived in rural or semi-rural areas in villages and small towns, but by 2030 it is projected that 60% of the world's population will live in urban areas. Areas, and the quality of life for future generations will inevitably be associated with the urban environment<sup>[13]</sup>.

It is also noticeable that the impact of climate change on different parameters can be increased in urban centers other than natural areas, possibly due to the creation of

urban thermal islands, making most of the urban areas warmer than the surrounding areas.

This study analyzes soil temperature change in the last three decades in the municipality of Novi Sad. The integrated remote-access approach has been successfully applied to determine the NDVI and LST changes using satellite images. Reduction of vegetation, spreading of the urban area ie. construction of new buildings, changes in land use patterns and other parameters were accompanied by the increase in the minimum and maximum LST of the surfaces. It was also attempted to identify newly constructed objects using a temperature difference, since it is assumed that temperatures would increase in such places. It turned out that this method is able to identify such sites, but that it is not reliable due to the fact that other land that has changed the way agricultural land is identified. After that, the temperature variation was analyzed depending on the alteration of the height difference. Then, using the regression analysis, it was attempted to determine the dependence between the NDVI and LST values. It turned out that there is some dependence, but there is no strong connection between these two values. All these changes indicate the rapid urbanization of the city of Novi Sad and the surrounding areas. This kind of study is therefore used to monitor urban expansion and other vegetation related phenomena.

In recent years, the application of heat data has been significantly increased in all types of Earth observation based on the application of research such as water management in agriculture, water resources management, crop evapotranspiration assessment, energy balance studies, climate change, hydrological cycle, vegetation monitoring, urban climate and ecological studies, etc.<sup>[7][17]</sup>. LST quickly varies with space and time due to the heterogeneity of surface parameters such as soil, water, vegetation, and therefore measurements on the ground are not reliable in wide areas. Remote reading can help us measure LST for a whole sphere with fine spatial and temporal resolution, not with exact observations.

## Acknowledgment

The authors thank the (<http://earthexplorer.usgs.gov/>) for providing the Landsat data used in this work free of cost through the internet.

## References

- [1] Carlson, T.N. and Ripley, D.A. On the relation between NDVI, fractional vegetation cover, and leaf area index. *Remote Sensing of Environment*, 1997, 2(3): 241–252.

- [2] Chander, G., Markham, B.L., Helder, D.L. Summary of current radiometric calibration coefficients for Landsat MSS, TM, ETM+, and EO-1 ALI sensors. *Remote Sensing of Environment*, 2009, 113(5): 893-903.
- [3] Danodia, A., Nikam, R. B., Kumar, S., Patel, N.R. Land surface temperature retrieval by radiative transfer equation and single channel algorithms using landsat-8 satellite data. *Indian Institute of Remote Sensing- ISRO*, 4- Kalidas road, Dehradun-248001, 2017.
- [4] Dos Santos, G.M., Meléndez-Pastor, I., Navarro-Pedreño, J., Gómez Lucas, I., A Review of Landsat TM/ETM based Vegetation Indices as Applied to Wetland Ecosystems. *Journal of Geographical Research*, 2019, 2(1): 35-49.
- [5] Easterling, D.R., Meehl, G.A., Parmesan, C., Changnon, S.A., Karl, T.R., Mearns, L.O. Climate extremes: observations, modeling, and impacts. *Science*, 2000, 289: 2068–2074.
- [6] Greenough, G., McGeehin, M., Bernard, S.M., Trtanj, J., Riad, J. and Engelberg, D. The potential impacts of climate variability and change on health impacts of extreme weather events in the United States. *Environmental Health Perspectives* 109 Suppl. 2, 2001, 191–198.
- [7] Kerr, Y.H., Lagouarde, J.P., Nerry, F., Otlé, C. Land surface temperature retrieval techniques and applications. In D. A. Quattrochi, & J. C. Luvall (Eds.), *Thermal remote sensing in land surface processes*. Boca Raton, Fla.: CRC Press, 2000: 33–109.
- [8] Li, Z.-L. and Becker, F. Feasibility of land surface temperature and emissivity determination from AVHRR data. *Remote Sensing of Environment*, 1993, 43(1): 67–85.
- [9] Mallick, J. Kant, Y., Bharat, B.D. Estimation of land surface temperature over Delhi using Landsat-7 ETM+. *Journal of Indian Geophysical Union*, 2008, 12(3): 131-140.
- [10] Nikam, B. R., Ibragimov, F., Chouksey, A., Garg, V., Aggarwal, S. P. Retrieval of land surface temperature from Landsat 8 TIRS for the command area of Mula irrigation project. *Environmental Earth Sciences*, 2016, 75: 1-17.
- [11] Pettorelli, N., Vik, J.O., Mysterud, A., Gaillard, J., Tucker, C.J., Stenseth, N.C. Using the satellite-derived NDVI to assess ecological responses to environmental change. *Trends in Ecology and Evolution*, 2005, 20: 503–510.
- [12] Popović, T., Đurđević, V., Živković, M., Jović, B., Jovanović, M. Promena klime u Srbiji“, Agencija za zaštitu životne sredine, Ministarstvo životne sredine i prostornog planiranja, Institut za meteorologiju, Fizički fakultet, Univerzitet u Beogradu, 2009.
- [13] Robinson, W.H. *Urban Insects and Arachnids: a Handbook of Urban Entomology*. Cambridge University Press, Cambridge, UK, 2005.
- [14] Rolston, H. *Conserving Natural Value*. Columbia University Press, New York, USA, 1994.
- [15] Rouse, J.W., Haas, R.H., Schell, J.A., Deering, D.W. Monitoring vegetation systems in the Great Plains with ERTS. *Proceedings of 3rd ERTS Symposium*, NASA SP-351 I, 1973: 309–317.
- [16] Saini, V. and Tiwari, K. Effect of urbanization on land surface temperature and NDVI: a case study of dehradun, India. *Conference: 38th Asian Conference on Remote Sensing*, New Delhi, 2017.
- [17] Sobrino, J. A., Jiménez-Muñoz, J. C., Paolini, L. Land surface temperature retrieval from LANDSAT TM 5. *Remote Sensing of Environment*, 2004, 90: 434-440.
- [18] Tucker, C. J. Red and photographic infrared linear combinations for monitoring vegetation. *Remote Sensing Environment*, 1979, 8: 127-150.
- [19] Valor, E. and Caselles, V. Mapping land surface emissivity from NDVI: application to European, African, and South American areas. *Remote Sensing of Environment*, 1996, 57(3): 167–184.
- [20] Van de Griend, A. A. and Owe, M. On the relationship between thermal emissivity and the normalized difference vegetation index for natural surfaces. *International Journal of Remote Sensing*, 1993, 14(6): 1119–1131.
- [21] Weng, Q., Lu, D., Schubring, J. Estimation of land surface temperature–vegetation abundance relationship for urban heat island studies. *Remote Sensing of Environment*, 2004, 89(4): 467-483.
- [22] Yu, X., Guo, X., Wu, Z. Land Surface Temperature Retrieval from Landsat 8 TIRS- Comparison between Radiative Transfer Equation-Based Method, Split Window Algorithm and Single Channel Method. *Remote sensing*, 2014, 6: 9829-9852.